Desalination and Water Treatment
www.deswater.com

doi: 10.5004/dwt.2020.24926

181 (2020) 346–354
March

Nano spinels of copper-doped cobalt aluminate ($Co_xCu_{(1-x)}Al_2O_4$) for removal of Cd(II) from aqueous solutions

Ali Shamsi, Saeedeh Hashemian*

Department of Chemistry, Yazd Branch, Islamic Azad University, Yazd, Iran, emails: Sa_hashemian@iauyazd.ac.ir (S. Hashemian), alishamsi@gmail.com (A. Shamsi)

Received 5 April 2019; Accepted 19 September 2019

ABSTRACT

The nano spinels of copper-doped cobalt aluminate ($Co_xCu_{(1-x)}Al_2O_4$, (x = 0–1)) have been synthesized by sol-gel method. The nano spinels were characterized by FTIR, X-ray diffraction, BET, transmission electron microscopy and scanning electronic microscopy methods. The adsorption of Cd(II) by nano spinels was studied. Results showed that adsorption efficiency of nano spinels is as follows: $Co_{0.5}Cu_{0.5}AlO_4$ > $Co_{0.3}Cu_{0.7}AlO_4$ > $Co_{0.7}Cu_{0.3}AlO_4$ > $CuAl_2O_4$ > $CoAl_2O_4$. Experimental results demonstrated that Cd(II) effectively removed by nano spinels in 90 min and solution pH of 6. Cd(II) removal was followed by the pseudo-first-order kinetic model. The equilibrium adsorption of Cd(II) was best described by the Langmuir isotherm model with maximum adsorption capacity (q_{max}) of 145 mg g^{-1} for $Co_{0.5}Cu_{0.5}AlO_4$. Results of thermodynamic studies revealed that adsorption of Cd(II) on nano spinels is an endothermic process. The studies clearly demonstrated that the nano spinels of $Co_xCu_{(1-x)}Al_2O_4$ could be an efficient and reusable sorbent for treatment of Cd(II) contaminated wastewaters. The desorption studies showed that the regeneration of $Co_{0.5}Cu_{0.5}AlO_4$ adsorbent can be easily achieved by inorganic acids. Results showed that the order of acids was as follows: nitric acid > hydrochloric acid > sulphuric acid > acetic acid.

Keywords: Adsorption; Cd(II); $CoAl_2O_4$; $CuAl_2O_4$; Nano spinel; $Co_xCu_{(1-x)}Al_2O_4$

1. Introduction

Due to high development of industrial activity in recent years, the levels of heavy metals in water system have noticeably increased over time. This makes it essential to develop methods that allow one to detect, quantify and remove heavy metals from the wastewaters. The different industries such as electro-plating, dyeing, plastic, battery and refining industry release these metals into aquatic environments [1,2]. Among these metal ions, Cd, Zn, Hg, Pb, Cr, Cu, etc. gain importance due to their high toxic nature even at very low concentrations. Cadmium, one of the most toxic heavy metals usually found in contaminated ecosystems. Heavy metal ions are not biodegradable, and they tend to collect in the organisms and enter the food chains through various pathways. Therefore, development of economically feasible techniques to remove heavy metals from the environment is in order. Various methods are available to remove these heavy metals from the environment. The classical physico-chemical methods employed to remove toxic metals, viz. precipitation, evaporation, ion exchange, and oxidation/reduction, pose severe constraints associated with high capital and operating costs, in addition to generating several by-products [3–5]. Adsorption is known as an effective and economic method for heavy metal removal. Adsorption is one of the easiest, safe and cost-effective methods, being widely used in effluent treatment processes [6]. Recently, there is an increasing interest in the

* Corresponding author.

use of high efficient adsorbents, which are able to remove metallic ions from aqueous solutions [7]. Removal of heavy metals by different sorbents such as chitosan [8], leaves [9], rice husk [10], activated carbon [11], magnetite [12,13], MgO [14], coconut shell [15], bentonite nano composite [16], cobalt silicate [17], sawdust of walnut [18] and carbon nanotubes [19] was studied.

The mixed metal oxides such as spinel structure oxides (AB_2O_4) constitute one of the most interesting classes of inorganic metalloid materials. They have fundamental physical and chemical properties. Among the spinel oxides, copper and cobalt aluminates possess interesting properties for technological application. Cobalt aluminate oxide ($CoAl_2O_4$) has been employed in various fields such as ceramic pigment, optical properties, catalysts in reactions, photo catalyst for degradation of pollutants such as carbon monoxide, sensors for gas and volatile organic compounds, hydrogenation, and removal of H_2S and NH_3 [20–26]. Some of the altered spinel ferrites were used as adsorbent [27–30]. The spinels mostly were used for dye removal. The some metal oxides and their composites were used for Cd removal [31–33]. Recently the composite of $NiFe_2O_4$ spinel was used for Cd removal [34].

The aim of this study was to prepare the nano spinels of copper-doped cobalt aluminates. The usage and adsorptive properties of nanocrystals for Cd(II) removal from aqueous solutions was the second aim.

2. Experimental

2.1. Materials and methods

All of the compounds were analytical grade and were used as received without any purification. All of the chemicals were purchased from Merck Chemical Co., (Germany). Distilled water was used in all of experiments.

The stock solution 1,000 mg L^{-1} of Cd(II) ions was prepared by dissolving metal salt from Cd $(NO_3)_2{\cdot}6H_2O$. The required diluted solutions with different concentrations were prepared by this stock solution.

$CuAl_2O_4$ and $CoAl_2O_4$ powders were prepared from aluminum nitrate ($Al(NO_3)_3{\cdot}9H_2O$), cobalt nitrate ($Co(NO_3)_2{\cdot}6H_2O$) and copper nitrate ($Cu(NO_3)_2{\cdot}3H_2O$).

Appropriate amount of $Co(NO_3)_2{\cdot}6H_2O$ and $Al(NO_3)_3{\cdot}6H_2O$ with molar ratio of Co^{2+}:Al^{3+} 1:2 was dissolved in the distilled water and then titrated drop wise by 1 M NH_3 till the pH was 8.5 under fast magnetic stirring at 25°C. Then the prepared sample was filtered off, washed with distilled water and then dried in a furnace at 150°C for 6 h [5]. For preparation of $Co_xCu_{(1-x)}Al_2O_4$ different ratio moles of Co:Cu (x = 0.0–1) were used. The preparation method was as the same.

Adsorption experiments were conducted to investigate the influence of adsorption parameters such as contact time and ratio of Co:Cu, pH, adsorbent mass and initial concentration of Cd(II) by using nanocrystals of copper-doped cobalt aluminate ($Co_xCu_{(1-x)}Al_2O_4$) as adsorbent.

0.05 g of adsorbent was added in 50 mL Cd(II) sample on rotary shaker at a constant speed of 150 rpm. After different contact times (0–180 min), the sorbent was removed from the solution and the equilibrium concentration of the Cd(II) in the solution was determined with atomic absorption spectrometer. All experiments were carried out at room temperature (25°C ± 1°C). The adsorbent was separated by centrifugation in 10,000 rpm for 10 min and residual cadmium was analyzed.

The FTIR transmission spectra were taken with a tensor-27 of Bruker Co. (Germany), Infrared spectrometer using the KBr pellet from 4,000 to 400 cm^{-1}. All pH measurements were carried out with an ISTEK-720P (Germany) pH meter. The powder X-ray diffraction (XRD) studies were made on a Philips PW1840 (Netherlands) diffractometer using Ni-filtered Cu kα radiation and wavelength 1.54 Å. The average particle size and morphology of samples were observed by SEM using a Hitachi S-3500 (Japan) scanning electron microscopy. The transmission electron microscopy (TEM) was employed using transmission electron microscope (Zeiss - EM10C - 80 kV, Germany).

The amount of adsorbed Cd(II) was calculated from the difference between the initial and final solution concentrations. The concentration of cation in solution was measured by an atomic absorption spectroscope, Varian AA240. All the experiments were repeated four times, and the average results were given. Relative standard deviation (% RSD) was determined between 1.82% and 2.5% for every point at all the tests. The removal efficiency and adsorption capacity of Cd(II) were calculated according to the below equations, respectively. The percentage removal of Cd(II) by the hereby adsorbent is given by:

$$\%\ \text{Removal} = \frac{\left(C_0 - C_e\right)}{C_0} \times 100 \tag{1}$$

where C_0, C_e are denoted as the initial and equilibrium concentration (mg L^{-1}) of Cd(II), respectively.

The amount of equilibrium adsorption, q_e (mg g^{-1}), was calculated by:

$$q_e = \frac{\left(C_0 - C_e\right)V}{W} \tag{2}$$

where C_0 and C_e (mg L^{-1}) are the liquid-phase concentrations of Cd(II) at initial and equilibrium, respectively. V (L) is the volume of the solution and W (g) is the mass of dry sorbent used.

3. Results and discussions

3.1. Characterization

X-ray powder diffraction analysis was used to identify the crystal structure of $Co_xCu_{(1-x)}Al_2O_4$ samples. First effect of calcination temperature on the crystallinity of sample was experienced; therefore, cobalt aluminate sample was heated at different temperatures (100°C, 300°C, 600°C and 900°C). The XRD patterns are shown at Fig. 1. The results are shown with increasing of calcination temperature, cobalt aluminate sample had more crystal order and at 900°C cobalt aluminate had the highest crystallinity form. At this temperature cobalt aluminate sample showed the characteristic diffraction peaks at 2θ values of 31.19°, 36.74°, 44.69°, 55.49°, 59.19° and 65.4° corresponding to the [220], [311], [400], [422], [511] and [440] planes, respectively. These planes are associated

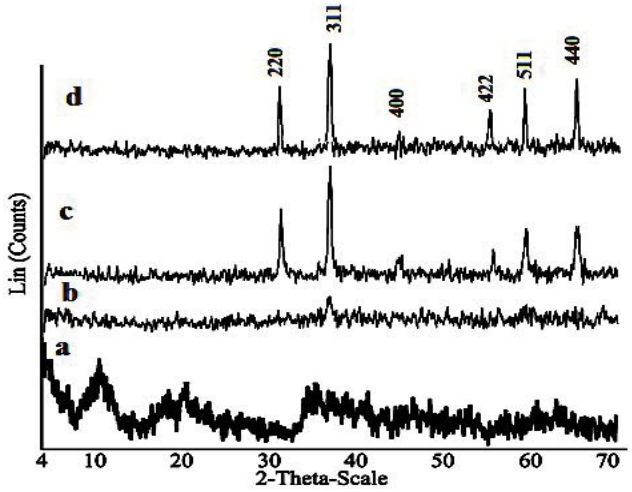

Fig. 1. XRD patterns of $CoAl_2O_4$ calcinated at (a) 100°C, (b) 300°C, (c) 600°C, and (d) 900°C.

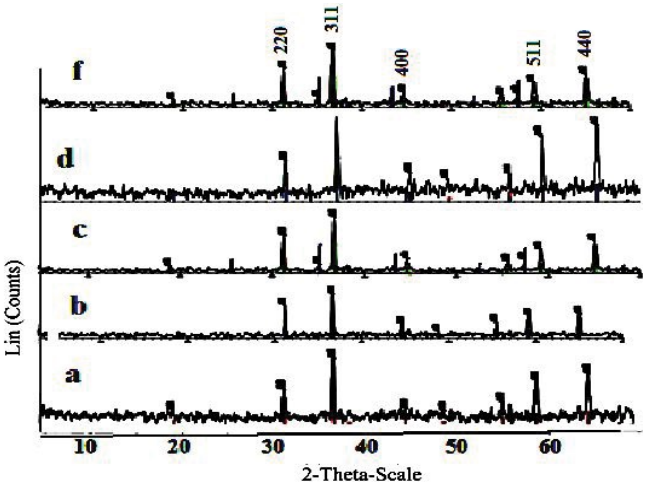

Fig. 2. XRD patterns of (a) $CoAl_2O_4$, (b) $Co_{0.7}Cu_{0.3}AlO_4$, (c) $Co_{0.5}Cu_{0.5}AlO_4$, (d) $Co_{0.3}Cu_{0.7}AlO_4$, and (e) $CuAl_2O_4$.

with the spinel type of $CoAl_2O_4$ with cubic structures in agreement with the Joint Committee on Powder Diffraction Standards (JCPDS) cards no. 44–0160. The XRD showed the formation of spinel phase at 900°C (2θ of 36.74° corresponding to d = 2.444) [35]. Cobalt aluminate sample also showed face centered cubic (FCC) with Fd-3m space group. However the spinel sample confirmed that the intensity of the peaks increases with increase in calcination temperature to 900°C.

The nanocrystals of spinel copper-doped cobalt aluminate $Co_xCu_{(1-x)}Al_2O_4$ (x = 0–1) were prepared and heated to 900°C. Typical XRD pattern for the samples of $Co_xCu_{(1-x)}Al_2O_4$ (where x = 0.0, 0.3, 0.5, 0.7 and 1.0) is shown in Fig. 2. Results of Fig. 2 show that the doping of copper on the cobalt aluminate did not change crystal spinel phase. The results of X-ray crystallographic showed the cubic unite cell ($a = b = c$ = 8.02) for $CoAl_2O_4$. Doping of Cu increases the lattice parameters of $CoAl_2O_4$ from 8.02 Å for $CoAl_2O_4$ to 8.08, 8.14, 8.18 and 8.2 Å for $Co_{0.3}Cu_{0.7}Al_2O_4$, $Co_{0.5}Cu_{0.5}Al_2O_4$, $Co_{0.7}Cu_{0.3}Al_2O_4$ and $CuAl_2O_4$, respectively. It is observed that the lattice parameters increase linearly with increase in copper concentration. The reason for this increase of lattice parameter values may be due to the larger ionic radii of Cu^{2+} (73 pm) as compared with Co^{2+} (70 pm).

The mean crystallite size (D) of the particles was calculated from the XRD line broadening measurement using the Scherrer equation:

$$D = \frac{0.89\lambda}{\beta \cos\theta} \tag{3}$$

where λ is the wavelength (Cu-Kα), β is the full width at the half maximum of the $Co_xCu_{(1-x)}Al_2O_4$ (311) line and θ is the diffraction angle. On the basis of the Scherrer equation, the main crystallite size was calculated 52, 35 and 46 nm for $CoAl_2O_4$, $Co_{0.5}Cu_{0.5}Al_2O_4$ and $CuAl_2O_4$, respectively.

FTIR spectra of as prepared spinels of $Co_xCu_{(1-x)}Al_2O_4$ were recorded from 4,000 to 500 cm^{-1}. The two main broad metal-oxygen bands are important in the IR spectra of all spinels. The highest IR band, V_1, is generally observed in the higher frequency range of 630–670 cm^{-1}, corresponding to the intrinsic stretching vibrations of the metal-oxygen bond at the tetrahedral site (M tetra-O). The lowest IR band, V_2, is usually observed in the frequency range of 450–385 cm^{-1}, assigned to stretching vibrations of the metal oxygen bond at the octahedral site (M octa-O). In the FTIR spectra, V_1 (640 cm^{-1}) for $CoAl_2O_4$ shifted slightly to higher frequencies (670 cm^{-1}) by replacing Co^{+2} ion with a Cu^{+2} ion. Small shifts of the V_1 peak positions indicate that changes due to the Co^{+2} substitution has slightly affected the metal-oxygen force constants in the tetrahedral site. This can be explained by the very small difference in both the atomic mass and ionic radii of the Cu and Co ions.

The surface morphology of $Co_xCu_{(1-x)}Al_2O_4$ (x = 0, 0.5, 1) was studied by scanning electronic microscopy (SEM) and results are shown in Fig. 3. The SEM micrographs showed spherical homogenous phase, uniformly distributed particles and highly porous morphology. Copper particles are brighter and $CoAl_2O_4$ nanoparticles are darker color in Fig. 3b.

TEM image of nanocrystals of spinel copper-doped cobalt aluminate is shown in Fig. 4. The TEM images showed particles size of 54, 35 and 43 nm for $CoAl_2O_4$, $Co_{0.5}Cu_{0.5}Al_2O_4$ and $CuAl_2O_4$, respectively.

The N_2 adsorption–desorption isotherm of $Co_xCu_{(1-x)}Al_2O_4$ nanoparticles is determined. The BET results of $Co_xCu_{(1-x)}Al_2O_4$ nanoparticles are shown in Table 1. Results also shown the surface area of nanoparticles was increased with increasing different amounts of Cu in doped cobalt aluminate.

3.2. Adsorption study

Foreknowledge of optimal conditions would allow a better design and modeling of the process. Thus the effect of some major parameters such as pH, contact time and amount of copper, amount of adsorbent and concentration of adsorbate was studied using the batch experiments.

3.2.1. Effect of contact time and copper contain of cobalt aluminate

To find an appropriate contact time between the sorbent and Cd metallic ion solution, adsorption capacities of metal

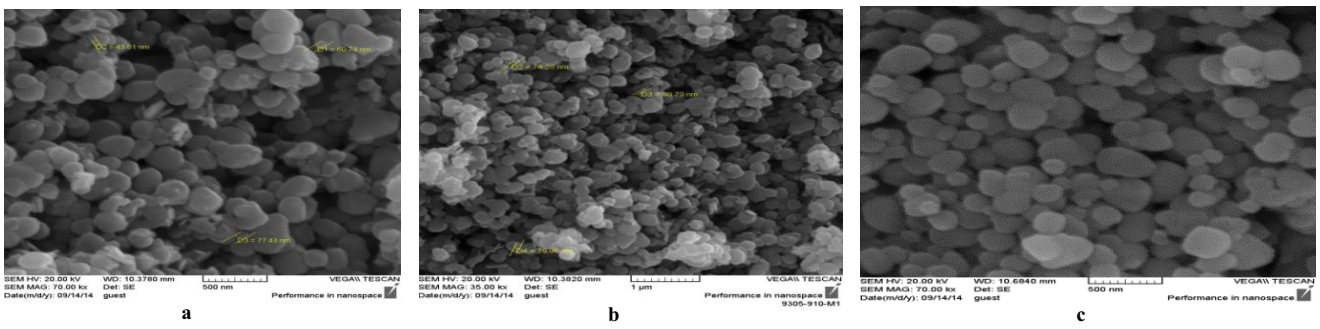

Fig. 3. SEM of (a) $CoAl_2O_4$, (b) $Co_{0.5}Cu_{0.5}Al_2O_4$, and (c) $CuAl_2O_4$ nanoparticles.

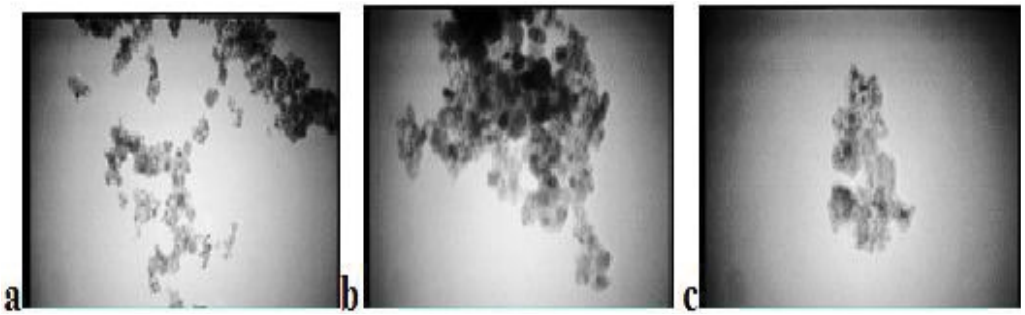

Fig. 4. TEM image of (a) $CoAl_2O_4$, (b) $Co_{0.5}Cu_{0.5}AlO_4$, and (c) $CuAl_2O_4$ nanoparticles.

Table 1
BET results of $Co_xCu_{(1-x)}Al_2O_4$ nanoparticles

Sample	Mean pore diameter (nm)	Total pore volume ($cm^3\ g^{-1}$)	Area ($m^2\ g^{-1}$)
$CoAl_2O_4$	48	7.83	285
$Co_{0.7}Cu_{0.3}Al_2O_4$	46	8.62	293
$Co_{0.5}Cu_{0.5}Al_2O_4$	37	9.30	323
$Co_{0.3}Cu_{0.7}Al_2O_4$	42	8.85	325
$CuAl_2O_4$	38	8.94	330

ion were measured as a function of time. The effect of equilibration time on the adsorption of Cd(II) ions was analyzed over a range of 0–240 min (Fig. 5). The plot reveals that the rate of the percentage of Cd removal is higher at the beginning. That is probably due to the larger surface area of the spinel sorbent being available at the beginning of process for the adsorption of metal. This shorter time indicates easier approachability of the binding sites for metal ions at the surface of nanoparticles of spinel sorbent. The removal of Cd(II) ions increased rapidly with time up to 90 min and thereafter increased slowly. According to the results, the equilibrium reached at 90 min and was taken as optimal contact time for the subsequent experiments, thereafter; it reached a constant value indicating that no more Cd(II) ions were further removed from solution as shown in Fig. 5.

Effect of copper contain of cobalt aluminate also was investigated. From Fig. 4, it looks copper had catalytic effect for $CoAl_2O_4$ and existence of copper increased the adsorption property of cobalt aluminate for Cd removal. The results showed that adsorption capability of nano spinel particles for

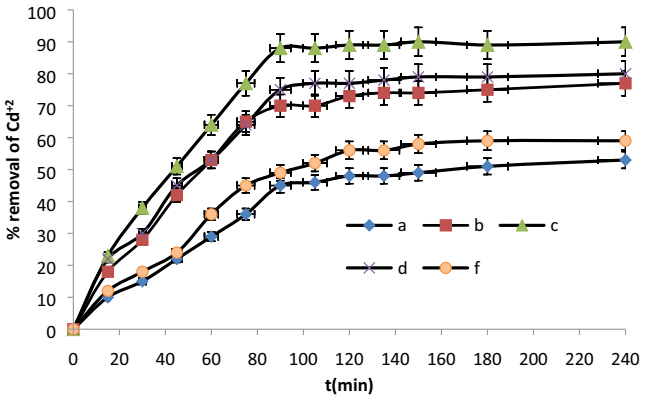

Fig. 5. Effect of contact time on the adsorption of Cd onto (a) $CoAl_2O_4$, (b) $Co_{0.7}Cu_{0.3}AlO_4$, (c) $Co_{0.5}Cu_{0.5}AlO_4$, (d) $Co_{0.3}Cu_{0.7}AlO_4$, and (f) $CuAl_2O_4$.

Cd(II) was as follows: $Co_{0.5}Cu_{0.5}AlO_4 > Co_{0.3}Cu_{0.7}AlO_4 > Co_{0.7}Cu_{0.3}AlO_4 > CuAl_2O_4 > CoAl_2O_4$.

3.2.2. Effect of pH on adsorption of Cd(II)

It is well known that adsorption of heavy metal ions depends on pH of aqueous solution. The pH of aqueous media is an important parameter controlling adsorption processes of heavy metals. The percentage removal of cadmium as a function of equilibrium pH was investigated for contact time of 90 min. pH was adjusted by adding 1.0 M HCl or 1.0 M NaOH. Fig. 6 indicates the effect of pH on the adsorption of

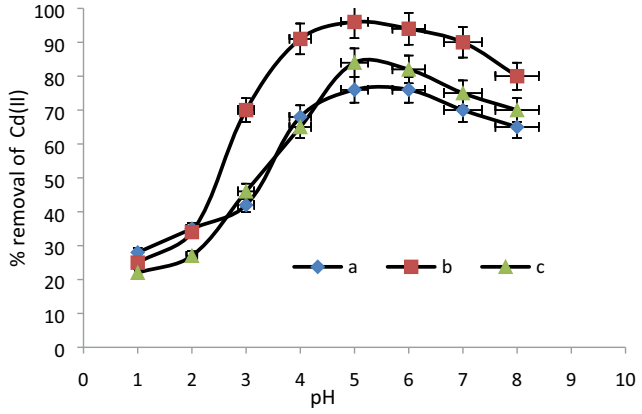

Fig. 6. Effect of pH for adsorption of Cd(II) by (a) $CoAl_2O_4$, (b) $Co_{0.5}Cu_{0.5}AlO_4$, and (c) $CuAl_2O_4$.

Cd(II) by $Co_xCu_{(1-x)}Al_2O_4$ nano spinels. At pH < 4.0, the Cd removal is low whereas it increased abruptly in the pH range from 4.0 to 6.0. At pH ≤ 3.0, H^+ ions compete with Cd(II) ions for adsorption on the sites in the adsorbent, which would hinder Cd(II) ions from reaching the binding sites of the sorbent caused by the repulsive forces. However, the metal removal is minimum presumably due to the enhanced competition of proton with cadmium ions. The removal of Cd(II) increased rapidly at pH values between 4.0 and 6.0.The increase in metal removal as pH increased can be explained on the basis of a decrease in competition between proton (H^+ or H_3O^+) and positively charged metal ions [M^{2+} and $M(OH)^+$] at the surface sites. The percentage removal of Cd^{2+} ions reached to 95% at pH 6 for $Co_{0.5}Cu_{0.5}AlO_4$. At pH ~ 6, the differences in removal by cadmium onto $Co_xCu_{(1-x)}Al_2O_4$ are obvious. At pH > 6.0, the Cd(II) ions get precipitated due to hydroxide anions forming a cadmium hydroxide precipitate. For this reason, the optimal pH value was selected to be 6.0 [36,37].

3.2.3. *Effect of initial Cd(II) concentration*

The effect of initial Cd concentration on the adsorption process was investigated. Fig. 7 indicates the effect of initial metal concentration on the adsorption of Cd(II) from 25 to 250 mg L^{-1} by spinel sorbents. By increasing the initial concentration of Cd(II) solution from 25 to 50 mg L^{-1}, the amount adsorbed increased. This may be attributed to an increase in the driving force of the concentration gradient with the increase in the initial Cd(II) concentration in order to overcome all mass transfer resistance of Cd(II) ions between the aqueous and solid phases. The initial concentration of Cd(II) solution from 50 to 250 mg L^{-1} decreased the present removal. Therefore, higher initial concentration of Cd(II) ions may decrease the adsorption capacity [38]. The initial concentration of 50 mg L^{-1} for next experiments was selected.

3.3. *Adsorbent dosage effect*

Adsorbent dosage is one of the important parameter of adsorption. The effect of adsorption dosage from 0.01 to 0.3 g was determined at initial metal ions concentration

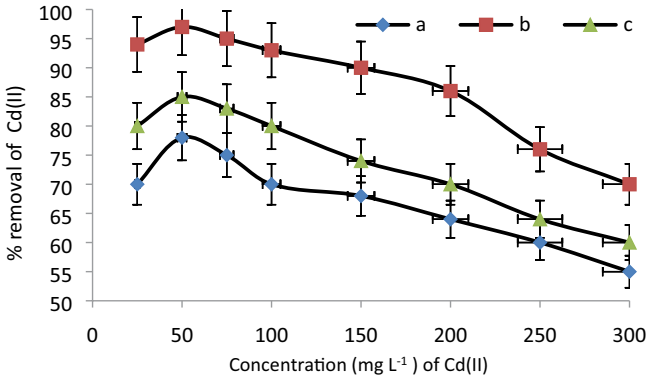

Fig. 7. Effect of initial concentration of Cd(II) by nano spinel sorbents (a) $CoAl_2O_4$, (b) $Co_{0.5}Cu_{0.5}AlO_4$, and (c) $CuAl_2O_4$.

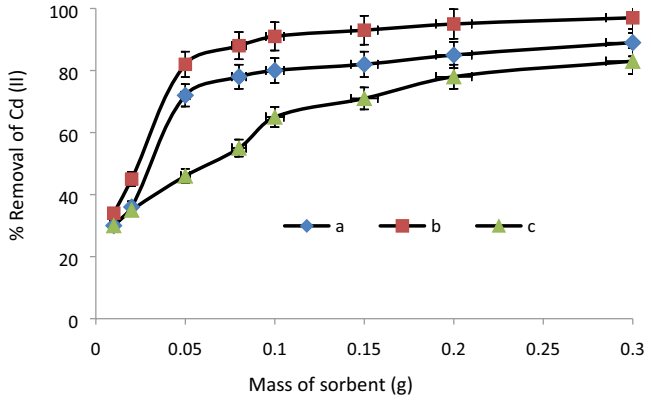

Fig. 8. Effect of adsorbent concentration on Cd(II) removal by (a) $CoAl_2O_4$, (b) $Co_{0.5}Cu_{0.5}AlO_4$, and (c) $CuAl_2O_4$.

of 50 mg L^{-1} and pH 6. The results of the investigations of cadmium removal are presented in Fig. 8. With the increase in dosage of spinel adsorbent, the percentage of adsorption increased from 0.01 to 0.1 g. This effect can be due to some of the adsorption sites remaining unsaturated during the adsorption reaction. At the initial step usually, there is fast increase in adsorption of Cd^{2+} with corresponding increase in adsorbate concentration which may be attributed to the increasing presence of adsorption sites. However, as the binding sites of the sorbent get saturated the curves level off due to the independence of the adsorption on concentration of the adsorbate. Therefore, best dosage of spinel sorbent was 0.05–0.1 g.

3.4. *Adsorption isotherms, kinetics and mechanism*

Various adsorption kinetic models have been used to describe the adsorption of metal ions. The first-order kinetic process has been used for reversible reaction with an equilibrium being established between liquid and solid phases. The pseudo-first-order rate by Lagergren has also widely been used. The adsorption rate expression of Lagergren is [39] as follows:

$$\mathrm{Ln}\,(q_e - q_t) = \ln q_e - k_1 t \quad (4)$$

where q_e is the amount adsorbed (mg g^{-1}) at equilibrium, q_t is the amount adsorbed (mg g^{-1}) at time t and k_1 is the adsorption rate constant (min^{-1}). The rate constants k_1, q_e and correlation coefficients R^2 were calculated using the slope and intercept of plots of $\ln(q_e - q_t)$ vs. t (Fig. 9a).

The kinetic data were further analyzed with Ho and McKay's [40] pseudo-second-order kinetics model. This model is based on the assumption that the adsorption follows second-order chemiadsorption. Its integrated linear form can be expressed as:

$$\frac{t}{q_t} = \frac{t}{q_e} + \frac{1}{\left(k_2 q_e^2\right)} \tag{5}$$

where q_e and q_t (mg g^{-1}) are the adsorption capacity at equilibrium and time t, k_2 (g mg^{-1} min) is the rate constant of the pseudo-second-order adsorption. The rate constants k_2, q_e and correlation coefficients R^2 were calculated from the linear plots of t/q_t vs. t (Fig. 9b). The R^2 value was significant in this case, which showed that adsorption of Cd(II) followed a pseudo-second-order kinetic model. This implied that adsorption in this case took place through chemical bond formation (chemisorption). Table 2 shows the kinetic parameters of Cd removal by spinel sorbents.

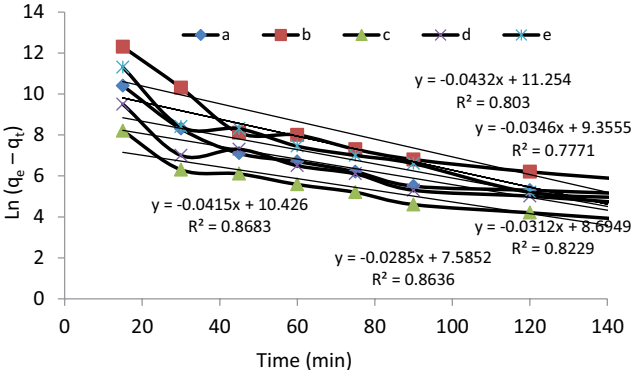

(a)

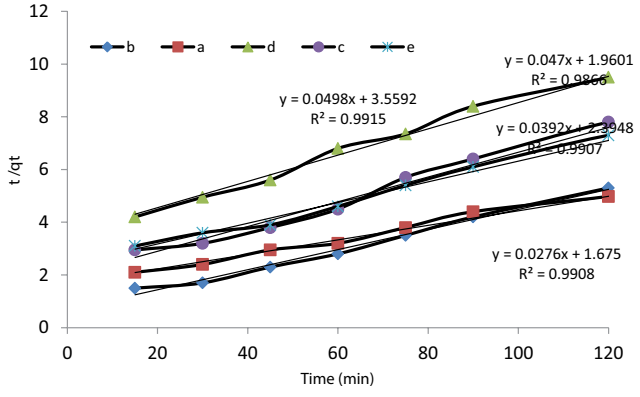

(b)

Fig. 9. (A) Pseudo-first-order kinetics for adsorption of Cd(II) onto removal by (a) $CoAl_2O_4$, (b) $Co_{0.7}Cu_{0.3}AlO_4$, (c) $Co_{0.5}Cu_{0.5}AlO_4$, (d) $Co_{0.3}Cu_{0.7}AlO_4$, and (e) $CuAl_2O_4$ (50 mL of Cd(II) 50 mg L^{-1}, pH 6, 0.1 g sorbent). (B) Pseudo-second-order kinetics for adsorption of Cd(II) onto removal by (a) $CoAl_2O_4$, (b) $Co_{0.7}Cu_{0.3}AlO_4$, (c) $Co_{0.5}Cu_{0.5}AlO_4$, (d) $Co_{0.3}Cu_{0.7}AlO_4$, and (e) $CuAl_2O_4$ (50 mL of Cd(II) 50 mg L^{-1}, pH 6, 0.1 g sorbent).

3.5. Adsorption isotherms

In order to recognize the design of an adsorption method, it is important to perform the study of equilibrium curves. In this study, two adsorption isotherms such as Langmuir and Freundlich adsorption isotherm models were used to describe the obtained equilibrium data.

Langmuir isotherm can be arranged in its linear form as following [41]:

$$\frac{C_{eq}}{q_{eq}} = \frac{1}{\left(q_{max} K_L\right)} + \frac{C_{eq}}{q_{max}} \tag{6}$$

where q_{eq} is the amount of adsorbed Cd(II) in the adsorbent (mg g^{-1}), C_{eq} is the equilibrium ion concentration in solution (mg L^{-1}), K_L (L mg^{-1}) is the equilibrium constant related to the adsorption energy, and q_{max} is the maximum adsorption capacity (mg g^{-1}).

The Freundlich isotherm assumes heterogeneous surface energies, in which the energy term in the Langmuir equation varies as a function of the surface coverage [38]. The adsorption data were also fitted to Freundlich isotherm, which is described by the linear form following the equation [42]:

$$\log q_{eq} = \log K_F + \left(\frac{1}{n}\right) \log C_{eq} \tag{7}$$

where K_F and n are the Freundlich constants; C_{eq} is the equilibrium ion concentration in solution (mg L^{-1}). According to Eq. (7), the values of K_F and n can be determined experimentally by plotting $\log q_{eq}$ vs. $\log C_{eq}$.

The high value of the regression correlation coefficient of Langmuir adsorption isotherm was obtained, which indicated a good agreement between the experimental values.

Table 3 shows the Langmuir and Freundlich equilibrium parameters for the adsorption of cadmium on $Co_xCu_{1-x}AlO_4$ nano spinels. It would be seen from the table that the Langmuir isotherms are linear with correlation coefficient R^2 in the range of 0.95–0.98. The maximum adsorption capacity observed for $Co_{0.5}Cu_{0.5}Al_2O_4$ was 145 mg g^{-1}.

Table 2
Kinetics parameters for the removal of Cd(II) onto $Co_xCu_{1-x}AlO_4$ (x = 0–1) nanoparticles

Sample	First order		Second order	
	R^2	k_1 (s^{-1})	R^2	k_2 (g mg^{-1} min^{-1})
$CoAl_2O_4$	0.777	3.46×10^{-2}	0.998	4.56×10^{-4}
$Co_{0.7}Cu_{0.3}Al_2O_4$	0.863	2.85×10^{-2}	0.994	2.14×10^{-3}
$Co_{0.5}Cu_{0.5}Al_2O_4$	0.803	4.32×10^{-2}	0.986	1.12×10^{-3}
$Co_{0.3}Cu_{0.7}Al_2O_4$	0.823	3.12×10^{-2}	0.991	6.96×10^{-4}
$CuAl_2O_4$	0.868	4.15×10^{-2}	0.99	6.42×10^{-4}

Table 3
Langmuir and Freundlich constants for the adsorption of Cd(II) onto $Co_xCu_{1-x}AlO_4$ (x = 0–1) nanoparticles

	Freundlich			Langmuir		
Sorbent	K_F	N	R^2	q_m mg g^{-1}	K_L L mg^{-1}	R^2
$CoAl_2O_4$	125	1.2	0. 83	85	32.5	0.96
$Co_{0.7}Cu_{0.3}Al_2O_4$	250	3.4	0.81	92	34.7	0.95
$Co_{0.5}Cu_{0.5}Al_2O_4$	345	2.8	0.86	145	38	0.98
$Co_{0.3}Cu_{0.7}Al_2O_4$	463	3.8	0.80	124	36.2	0.97
$CuAl_2O_4$	542	6.4	0.82	98	34.3	0.97

3.6. Thermodynamic studies

The thermodynamic parameters for Cd adsorption onto spinel sorbents have been calculated. The thermodynamic parameters, change in the standard free energy ($\Delta G°$), enthalpy ($\Delta H°$) and entropy ($\Delta S°$) associated with the adsorption process. The Gibbs free energy change $\Delta G°$ of adsorption process can be calculated from classic Van't Hoff equation [43]:

$$\Delta G° = -RT \ln K_C \tag{8}$$

where R is the universal gas constant (8.314 J mol^{-1} K^{-1}), T is the absolute temperature, and K_C is the equilibrium constant. The apparent equilibrium constant of the sorption, K_C is the equilibrium constant of Van't Hoff equation. K_C is obtained from:

$$K_C = \frac{C_A}{C_s} \tag{9}$$

where K_C is the equilibrium constant, C_A is the amount of Cd(II) adsorbed on the adsorbent of solution at equilibrium (mg L^{-1}), and C_S is the equilibrium concentration of Cd(II) in the solution (mg L^{-1}).

The enthalpy change ($\Delta H°$) (i.e., heat of adsorption) and entropy change ($\Delta S°$) is related with the Gibbs free energy by the equation:

$$\ln K_C = \frac{\Delta G°}{RT} = \frac{\Delta H°}{RT} + \frac{\Delta S°}{R} \tag{10}$$

A plot ln K_C vs. (1/T) gives a straight line, $\Delta H°$ and $\Delta S°$ can be determined from intercept and slope, respectively.

The negative values of $\Delta G°$ indicated thermodynamically feasible and spontaneous nature of the adsorption of Cd(II) by nanoparticles of spinel sorbent. The decrease in negative $\Delta G°$ values together with an increase in temperatures shows an increase in feasibility of sorption at higher temperatures. The negative $\Delta H°$ indicates the exothermic nature of the sorption process. The $\Delta H°$ and $\Delta S°$ values for $Co_{0.5}Cu_{0.5}Al_2O_4$ were found –7.3 kJ mol^{-1} and 46 J mol^{-1} K^{-1}, respectively. The positive values of entropy disclosed the increasing of randomness at the solid/liquid interface, suggesting the affinity of Cd ions on the surface of ferrite adsorbents [44]. Table 4 shows thermodynamic parameters for Cd adsorption onto $Co_xCu_{1-x}AlO_4$ sorbents.

Table 4
Thermodynamic parameters for adsorption of Cd(II) by adsorption onto $Co_xCu_{1-x}AlO_4$ (x = 0–1) nanoparticles

Sample	T (K)	$\Delta G°$ (kJ mol^{-1})	$\Delta H°$ (kJ mol^{-1})	$\Delta S°$ (J mol^{-1} K^{-1})
$CoAl_2O_4$	303	–15.387	–5.6	32.3
	313	–15.70		
	323	–16.0		
	333	–16.36		
$Co_{0.7}Cu_{0.3}Al_2O_4$	303	–16.9	–6.22	35.3
	313	–17.27		
	323	–17.62		
	333	–17.97		
$Co_{0.5}Cu_{0.5}Al_2O_4$	303	–21.24	–7.3	46
	313	–21.7		
	323	–22.16		
	333	–22.62		
$Co_{0.3}Cu_{0.7}Al_2O_4$	303	–19.36	–6.6	42
	313	–19.74		
	323	–20.167		
	333	–20.59		
$CuAl_2O_4$	303	–18.14	–6.9	38
	313	–18.8		
	323	–19.17		
	333	–19.55		

3.7. Regeneration of spinel sorbent

The adsorption capacity of the $Co_{0.5}Cu_{0.5}Al_2O_4$ nano spinel for Cd(II) after its regeneration has also been studied. The spent nano spinel was regenerated following the process mentioned above. Experiments on adsorption desorption and regeneration of nano spinel was performed with batch method. Thus, the Cd(II) ions are recovered and the nano spinel can be reused many times for desorption. Once the adsorption process had been finished, the centrifuged solids were washed with some drops of double distilled water to dilute and remove residual solution. Commonly, it is known that heavy metals can be separated from nano spinel by desorption in an inorganic acid or alkaline medium. Therefore, nitric acid, hydrochloric acid, sulphuric acid and acetic acid 0.1 M were verified for desorption. 50 mL of 50 mg L^{-1} of Cd solution at pH 6 stirred for 90 min for $Co_{0.5}Cu_{0.5}Al_2O_4$ nanoparticles. The mixture was stirred at 150 rpm in an orbital shaker at 25°C for 90 min. After the filtration, the residue was treated with different acids. Among them 0.1 M nitric acid gave the most effective result releasing about 90% of metal ions onto the solution in four successive cycles. Results are shown in Fig. 10. Results showed that the order of acids was as follows: nitric acid > hydrochloric acid > sulphuric acid > acetic acid. Therefore, HNO_3 was selected as a regenerating agent [45].

4. Conclusion

In this work, the nanosized spinels of $Co_xCu_{(1-x)}Al_2O_4$ were successfully prepared. The XRD patterns and FTIR

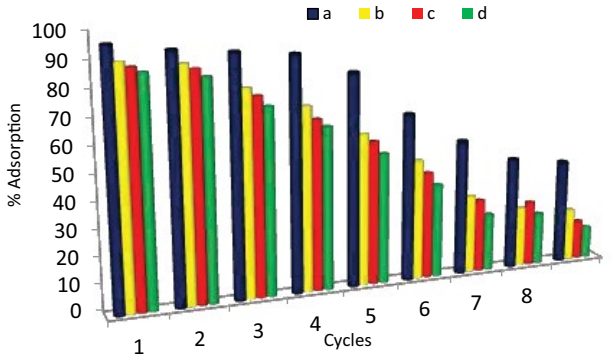

Fig. 10. Regeneration of $Co_{0.5}Cu_{0.5}Al_2O_4$ by (a) nitric acid, (b) hydrochloric acid, (c) sulphuric acid, and (d) acetic acid.

spectroscopy confirmed the pure spinel phase formation for all samples. The SEM and TEM images showed that the nano spinels have spherical shapes with small agglomeration. The potential uses of nano spinels of $Co_xCu_{(1-x)}Al_2O_4$ as adsorbent for the removal of Cd(II)ions as a heavy metal from synthetic wastewater was investigated. The maximum cadmium 50 mg L^{-1} adsorbed at contact time of 90 min and pH 6. It was seen that these spinel ferrites are very efficient for removal of Cd(II).

Adsorption of Cd(II) ions depends on their initial concentrations, pH and contact time.

Adsorption process was followed by the pseudo-first-order kinetic model and isothermal data of adsorption on sorbent can be modeled by Langmuir isotherm. Desorption process was performed and HNO_3 was selected as a regenerating agent.

Acknowledgment

The authors wish to express their gratitude to Islamic Azad University-Yazd branch for the support of this work.

References

[1] A. Roy, J. Bhattacharya, Removal of Cu (II), Zn (II) and Pb (II) from water using microwave-assisted synthesized maghemite nanotubes, Chem. Eng. J., 211 (2012) 493–500.
[2] V.K. Gupta, A. Rastogi, Biosorption of lead(II) from aqueous solutions by non-living algal biomass *Oedogonium* sp. and *Nostoc* sp. a comparative study, Colloids Surf., B, 64 (2008) 170–178.
[3] F. Fu, Q. Wang, Removal of heavy metal ions from wastewaters: a review, J. Environ. Manage., 92 (2011) 407–418.
[4] Z. Aksu, Equilibrium and kinetic modeling of cadmium (II) biosorption by C. vulgaris in a batch system: effect of temperature, Sep. Purif. Technol., 21 (2001) 285–294.
[5] K.S. Rao, M. Mohapatra, S. Anand, P. Venkateswarlu, Review on cadmium removal from aqueous solutions, Inter. J. Eng. Sci. Technol., 2 (2010) 81–103.
[6] B.G. Alhogbi, M.A. Salam, O.I. Environmental remediation of toxic lead ions from aqueous solution using palm tree waste fibers biosorbent, Desal. Wat. Treat., 145 (2019) 179–188.
[7] P.S. Keng, S.L. Lee, S.T. Ha, Y.T. Hung, S.T. Ong, Removal of hazardous heavy metals from aqueous environment by low-cost adsorption materials, Environ. Chem. Lett., 12 (2014) 15–25.
[8] S.M. Nomanbhay, K. Palanisamy, Removal of heavy metal from industrial wastewater using chitosan coated oil palm shell charcoal, Electron. J. Biotechnol., 8 (2005) 1–7.
[9] A.H. Mahvi, J. Nouri, G.A. Omrani, F. Gholam, Application of *Platanus orientalis* leaves in removal of cadmium from aqueous solution, World Appl. Sci. J., 2 (2007) 40–44.
[10] S. Sobhanardakani, R. Zandipak, Adsorption of Ni (II) and Cd (II) from aqueous solutions using modified rice husk, Iran. J. Health Sci., 3 (2015) 1–9.
[11] K.L. Wasewar, P. Kumar, S. Chand, B.N. Padimini, T. Tow Teng, Adsorption of cadmium ions from aqueous solution using granular activated carbon and activated clay, Clean Soil Air Water, 38 (2010) 649–656.
[12] M. Hosseinzadeh, S.A. Seyyed Ebrahimi, S. Raygan, S.M. Masoudpanah, Removal of cadmium and lead ions from aqueous solution by nano crystalline magnetite through mechanochemical activation, J. Ultrafine Grained Nanostr. Mater., 49 (2016) 72–79.
[13] A.F. Ngomsik, A. Bee, M. Draye, G. Cote, V. Cabuil, Magnetic nano-and microparticles for metal removal and environmental applications: a review, Comptes. Rendus. Chim., 8 (2005) 963–970.
[14] C. Xiong, W. Wang, F. Tan, F. Luo, J. Chen, X. Qiao. Investigation on the efficiency and mechanism of Cd (II) and Pb (II) removal from aqueous solutions using MgO nanoparticles, J. Hazard. Mater., 299 (2015) 664–674.
[15] D.N. Olowoyo, A.O. Garuba, Adsorption of Cadmium Ions using activated carbon prepared from coconut shell, Global Adv. Res. J. Food Sci. Technol., 1 (2012) 81–84.
[16] S. Hashemian, H. Saffari, S. Ragabion, Adsorption of cobalt (II) from aqueous solutions by Fe_3O_4/bentonite nanocomposite, Water Air Soil Pollut., 226 (2015) 2212–2222.
[17] K. Parmar, Removal of cadmium from aqueous solution using cobaltsilicate precipitation tube (CoSPT) as adsorbent, Inter. J. Sci. Inv. Today, 2 (2013) 204–215.
[18] B. Yasemin, T. Zeki, Removal of heavy metals from aqueous solution by sawdust adsorption, J. Environ. Sci., 19 (2007) 160–166.
[19] Ihsanullah, A. Abbas, A.M. Al-Amer, T. Laoui, M.J. Al-Marri, M.S. Nasser, M. Khraisheh, M.A. Atieh, Heavy metal removal from aqueous solution by advanced carbon nanotubes: critical review of adsorption applications, Sep. Purif. Technol., 157 (2016) 141–161.
[20] X. Duan, M. Pan, F. Yu, D. Yuan, Synthesis, structure and optical properties of $CoAl_2O_4$ spinel nanocrystals, J. Alloys Comp., 509 (2011) 1079–1083.
[21] J.H. Kim, B.R. Son, D.H. Yoon, K.T. Hwang, H.G. Noh, W. Seok, Characterization of blue $CoAl_2O_4$ nano-pigment synthesized by ultrasonic hydrothermal method, Ceram. Int., 38 (2012) 5707–5712.
[22] M. Zayat, D. Levy, Blue $CoAl_2O_4$ particles prepared by the sol–gel and citrate–gel methods, Chem. Mater., 12 (2000) 2763–2769.
[23] M.C. Gardey Merino, A.L. Estrella, M.E. Rodriguez. L. Acuña, M. S. Lassa. G.E. Lascalea, Combustion syntheses of $CoAl_2O_4$ powders using different fuels, Proc. Mater. Sci., 8 (2015) 519–525.
[24] E. Escalona Platero, C. Otero Arean, J.B. Parra, Synthesis of high surface area $CoAl_2O_4$ and $NiAl_2O_4$ spinels by an alkoxide route, Res. Chem. Int., 25 (1999) 187–194.
[25] W. Li, J. Li, J. Guo, Synthesis and characterization of nano-crystalline $CoAl_2O_4$ spinel powder by low temperature combustion, J. Europ. Cer. Soc., 23 (2003) 2289–2295.
[26] E.J. Lim, S.Y. Jung, S.C. Lee, J.C. Kim, Enhancing the effect of $CoAl_2O_4$ on the simultaneous removal of H_2S and NH_3 on Co- and Mo- based catal-sorbents in IGCC, Sep. Purif. Technol., 177 (2017) 94–100.
[27] L.P. Lingamdinne, Y.Y. Chang, J.K. Yang, J. Singh, E.H. Choi, M. Shiratani, J.R. Koduru, P. Attri, Biogenic reductive preparation of magnetic inverse spinel iron oxide nanoparticles for the adsorption removal of heavy metals, Chem. Eng. J., 307 (2017) 74–84.
[28] B. Fang, Y. Yang, F. Wang, Z. Chu, X. Sun, J. Li, L. Wang, Adsorption of Pb (2+) from aqueous solution using spinel

ferrite prepared from steel pickling sludge, Water Sci. Technol., 73 (2016) 1112–1121.
[29] N. Sezgin, A. Yalçın, Y. Köseoğlu, $MnFe_2O_4$ nano spinels as potential sorbent for adsorption of chromium from industrial wastewater, Desal. Wat. Treat., 57 (2016) 16495–16506.
[30] D.H. Kumar Reddy, S.M. Lee, Three-dimensional porous spinel ferrite as an adsorbent for Pb(II) removal from aqueous solutions, *Ind. Eng. Chem. Res.*, 52 (2013) 15789–15800.
[31] A. Farrokhnia, N. Javadnia, The thermodynamic and kinetics study of removal of Cd(II) by nanoparticles of Cobalt oxide in aqueous solution, Iran. J. Chem. Chem. Eng., 38 (2019) 127–139.
[32] T.K. Naiya, A.K. Bhattacharya, S.K. Das, Adsorption of Cd(II) and Pb(II) from aqueous solutions on activated alumina, J. Colloid Interface Sci., 333 (2009) 14–26.
[33] M.N. Rashed, M.A. Eltaher, A.N.A. Abdou, Adsorption and photocatalysis for methyl orange and Cd removal from wastewater using TiO_2/sewage sludge-based activated carbon nanocomposites, R. Soc. Open Sci., 4 (2017) 170834.
[34] P. Kahrizi, F.S. Mohseni Shahri, F. Moeinpour, Adsorptive removal of cadmium from aqueous solutions using $NiFe_2O_4$/hydroxyapatite/graphene quantum dots as a novel nano adsorbent, J. Nano. Chem., 8 (2018) 441–452.
[35] M. Liusar, A. Fores, A. Badenes, J. Calbo, M.A. Tena, G. Monros, Colour analysis of some cobalt-based blue pigments, J. Europ. Ceramic Soc., 21 (2001) 1121–1130.
[36] R. Abu-El-Halawa, S.A. Zabin, Removal efficiency of Pb, Cd, Cu and Zn from polluted water using dithiocarbamate ligands, J. Taibah Univ. Sci., 11 (2017) 57–65.
[37] M.R. Mehrasbi, Z. Farahmandkia, B. Taghibeigloo, A. Taromi, Adsorption of Lead and Cadmium from aqueous solution by using almond shells, Water Air Soil Pollut., 199 (2009) 343–351.
[38] N.K.E.M. Yahaya, M.F. Pakir Mohamed Latiff, Ismail Abustan, O. Solomon Bello, M. Azmier Ahmad, Adsorptive removal of Cu (II) using activated carbon prepared from rice husk by $ZnCl_2$ activation and subsequent gasification with CO_2, Inter. J. Eng. Technol. IJET-IJENS, 11 (2011) 207–211.
[39] S. Lagergren, About the Theory of So-Called Adsorption of Soluble Substances, K. Sven. Vetensk. Handl., 24 (1898) 1–39.
[40] Y.S. Ho, G. McKay, Pseudo-second order model for sorption processes, Process Biochem., 34 (1999) 451–465.
[41] I. Langmuir, The Adsorption of gases on plane surfaces of glass, Mica and Platinum, J. Am. Chem. Soc., 40 (1918) 1361–1403.
[42] H.M.F. Freundlich, Over the adsorption in solution, J. Phys. Chem., 57 (1906) 385–470.
[43] S. Hashemian, M. Mirshamsi, Kinetic and thermodynamic of adsorption of 2-picoline by sawdust from aqueous solution, J. Ind. Eng. Chem., 18 (2012) 2010–2015.
[44] M.H. Salmani, M. Miri, M.H. Ehrampoush, A. Alahabadi, A. Hosseini-Bandegharaei, Comparing cadmium removal efficiency of a magnetized biochar based on orange peel with those of conventional orange peel and unmodified biochar, Desal. Wat. Treat., 82 (2017) 157–169.
[45] S. Lata, P.K. Singh, S.R. Samadder, Regeneration of adsorbents and recovery of heavy metals: a review, Int. J. Environ. Sci. Technol., 12 (2015) 1461–1478.